EUROPEAN WORKSHOP ON
ELECTROCHEMICAL TECHNOLOGY FOR MOLTEN SALTS

14÷17 March 1993, Sintra (Portugal)

INVESTIGATION ON THE KINETICS AND STABILITY OF NiO(Li) AND $La_{0.8}Sr_{0.2}CoO_3$ IN MOLTEN CARBONATES BY MEANS OF ELECTROCHEMICAL IMPEDANCE SPECTROSCOPY

L. GIORGI[1], M. CAREWSKA[1], E. SIMONETTI[1], S. SCACCIA[1], F.CROCE[2] and A. POZIO[2]

[1] ENEA, C.R.E. Casaccia, Via Anguillarese 301, 00060 S. Maria di Galeria (Rome), Italy
[2] University of Rome, Department of Chemistry, P.le A. Moro 5, 00185 Rome, Italy

INVESTIGATION ON THE KINETICS AND STABILITY OF NiO(Li) AND $La_{0.8}Sr_{0.2}CoO_3$ IN MOLTEN CARBONATES BY MEANS OF ELECTROCHEMICAL IMPEDANCE SPECTROSCOPY

L. GIORGI[1], M. CAREWSKA[1], E. SIMONETTI[1], S. SCACCIA[1], F.CROCE[2] and A. POZIO[2]

[1] ENEA, C.R.E. Casaccia, Via Anguillarese 301, 00060 S. Maria di Galeria (Rome), Italy
[2] University of Rome, Department of Chemistry, P.le A. Moro 5, 00185 Rome, Italy

Keywords: molten carbonates, nickel oxide, perovskite, impedance spectroscopy, oxygen electroreduction.

ABSTRACT

An investigation on the kinetic of oxygen electroreduction in molten carbonates was carried out; in particular the reaction mechanism on NiO (lithium doped) and $La_{0.8}Sr_{0.2}CoO_3$ was studied. The calculated reaction orders relative to O_2 and CO_2 induced to suppose that in the reaction rate determining step on NiO(Li) a peroxide intermediate is involved; instead on $La_{0.8}Sr_{0.2}CoO_3$ it was no possible to determine the reaction orders due to the instability of the electrodes. The perovskite structure evolves during the time, with the formation of a passive layer on the surface, the loss of strontium (doping element) and the reaction with the electrolyte support (γ-$LiAlO_2$).

INTRODUCTION

The molten carbonate fuel cells (MCFCs) are subjected to extensive investigations inside several research and development programs [1,2,3]. This interest is coming from the fact that such a device owns a very promising characteristics for the large-scale electrical power generation; MCFC joint a potentially very high efficiency with the capability to utilize a wide variety of fossil fuel the possibility of internal reforming [4], the high temperature heat cogeneration and a very high efficiency with a minimal pollution.

The electrochemical reactions, involved in the anodic hydrogen oxidation and cathodic oxygen reduction, are the following:

(1) $H_2 + CO_3^{2-} \Rightarrow H_2O + CO_2 + 2\,e^-$

(2) $0.5\,O_2 + CO_2 + 2\,e^- \Rightarrow CO_3^{2-}$

and the the final product is water

(3) $H_2 + 0.5\,O_2 \Rightarrow H_2O$

The carbonate ions, consumed at the anode and generated at the cathode, are continuously transferred through a porous ceramic matrix (γ-$LiAlO_2$) filled with an alkaline carbonates mixture.

The device state of art is:

a) an operating temperature ranging from 600 to 700 °C;
b) a porous nickel anode containing a suitable antisintering additive (usually chromium, alumina or aluminium);
c) a porous nickel oxide (in situ oxidized and lithiated);

d) a lithium aluminate matrix (tile) impregnated with an electrolyte composed by Li and K carbonates at the eutectic composition (Li/K=62/38 $\%_{mol}$) .

In a MCFC both the anodic and cathodic processes are very complex, mainly due to the fact that we are in presence of two bimodal porous gas-diffusing electrodes. As well known, in this type of electrodes the overall process is usually under mixed control (kinetics, mass transfer and ionic conduction). In this condition the determination of the rate limiting processes is a very hard task.

The kinetics of gas electrode reactions in molten carbonate are very important to understand the electrode processes in the MCFC. The experimental difficulties related to working in molten carbonate systems have restricted the evaluation of kinetic data to submerged flat electrodes in excess of electrolyte. The conditions of a porous gas diffusion electrode are quite different and it is important to verify the validity of the kinetic parameters also in these conditions.

The cathodic reaction has been extensively studied and many approaches have been utilised in the past, in order to establish the rate determining step (r.d.s.) and to obtain the numeric values of the reaction orders relative to O_2 and CO_2. The results reported in literature, both on flat [5,6,7,8,9] and porous [10,11,12] electrodes, are contradictory and the reaction mechanism for O_2 reduction in molten carbonates is not well understood.

The O_2 solubilization mechanisms in molten carbonates are chemical in nature, with the formation of peroxides (O_2^{2-}) and superoxides (O^{2-}). For this reason the mechanism of oxygen cathodic reduction is not completely clear, but it is possible to suppose three main pathways with different intermediate species: peroxide, superoxide and peroxymonocarbonate.

If the predominating ion is peroxide, the peroxide path (POP) is :

(4a) $2\ CO_3^{2-} + O_2 \Leftrightarrow 2\ O_2^{2-} + 2\ CO_2$

(4b) $O_2^{2-} + 2\ e^- \Rightarrow 2\ O^{2-}$ (r.d.s.)

(4c) $2\ O^{2-} + 2\ CO_2 \Leftrightarrow 2\ CO_3^{2-}$

In the case in which the superoxide ion is predominant, the superoxide path (SOP) is:

(5a) $2\ CO_3^{2-} + 3\ O_2 \Leftrightarrow 4\ O_2^{-} + 2\ CO_2$

(5b) $O_2^{-} + e^- \Rightarrow O_2^{2-}$ (r.d.s.)

(5c) $O_2^{2-} + 2\ e^- \Leftrightarrow 2\ O^{2-}$

(5d) $2\ O^{2-} + 2\ CO_2 \Leftrightarrow 2\ CO_3^{2-}$

Moreover, as an alternative to the previous mechanisms some authors [4,5] postulated the peroxy-monocarbonate path (POMCP):

(6a) $1/2\ O_2 + CO_3^{2-} \Leftrightarrow CO_4^{2-}$

(6b) $CO_4^{2-} + e^- \Rightarrow CO_3^{2-} + O^-$ (r.d.s.)

(6c) $O^- + e^- \Leftrightarrow O^{2-}$

(6d) $O^{2-} + CO_2 \Leftrightarrow CO_3^{2-}$

The SOP and POP mechanisms have been experimentally supported by ESR (electron spin resonance) determination of O_2^{2-} and O_2^- species on rapid quenched electrolyte [13]. On the contrary, there are no reported experimental evidences for the CO_4^{2-} ion presence in molten carbonate.

Following Appleby and Nicholson [6], it is possible to derive the relationship between the exchange current density (i_o) and the partial pressures of O_2 and CO_2 :

(7) $i_o = k\ pO_2^a\ pCO_2^b$

where a and b are, respectively, the reaction order relative to oxygen and carbon dioxide. In table 1 the theoretical reaction orders for the three different mechanisms are summarized.

Table 1 - Theoretical reaction orders for the oxygen electroreduction in molten alkaline carbonates (SOP=superoxide path, POP=peroxide path, POMCP=peroxi-monocarbonate path, a=reaction order relative to O_2, b=reaction order relative to CO_2).

mechanism path	a	b
SOP	0.625	-0.75
POP	0.375	-1.25
POMCP	0.375	-0.25

In the actual fuel cell electrodes the detailed study of the kinetics is further complicated by the electrode porosity, therefore it is very difficult to investigate a system like that. Such a complexity is due to the lack of knowledge about some properties of this system (i.e., electrolyte distribution inside the porous electrode, gas solubility in molten carbonates, activity of intermediate species, etc.). As a consequence, it is very difficult both to extract the kinetics parameters from experimental data and to predict the validity of the proposed models for porous electrodes [14,15].

Recently, Yuh and Selman [15] reported both the literature data on the kinetics reaction orders and their own experimental results obtained by "in-situ" electrochemical impedance spectroscopy on actual porous nickel electrodes utilizing a small scale 3-cm^2 laboratory cell. Their results show a large deviation from the theoretical value of the reaction orders, also if they affirm that their data are close to the superoxide path.

Another problem to solve for the development of MCFC technology is the slow, but constant, dissolution of NiO(Li) in the electrolyte [16,17,18]. As a consequence of this phenomenon, the cathodic material is dispersed and transported inside the electrolyte, due to the concentration gradients and electrical field in the tile.

In an actual MCFC, a concentration gradient for the oxygen inside the electrolyte is generated; such a concentration profile is going down from the cathode to the anode. Therefore, in particular regions between the electrodes, the pO_2 reaches values for which the NiO is stable [19]. In these zones the nickel equilibrium solubility decreases and the metallic nickel deposition is possible, due to the reduction by hydrogen coming from the anode. So, islands of metallic nickel precipitate inside the tile, and as a consequence a nickel gradient is present. This gradient produces a continuos transport of cathodic material from the electrode/electrolyte interface to the bulk of the electrolyte. Such a phenomenon shorts the cell life, both by internal shortcircuits and cathodic material depletion.

In answer to that problem it is necessary to develop new cathodic materials alternative to NiO(Li). Such materials must have the following requirements:

a) high electronic conductivity at 650 °C (σ>1 S/cm);
b) stability in the operative conditions of MCFC (650 °C, O_2/CO_2 mixture);
c) solubility in the cathode environment lower and in the anode one higher than NiO(Li);
d) high electrocatalytic activity for the O_2 reduction;
e) be suitable for the fabrication of porous electrodes with high specific surface area, porosity=70÷80 %, mean pore diameter=7÷15 μm.

Up to date, the most study carried out on alternative materials [20,21,22,23] were focused on the electronic conductivity, while very few information are available on the physical-chemical and electrochemical characteristics related to the fabrication procedures. For these reasons the results obtained by different authors often do not agree.

More than 50 ceramic compounds were considered as alternative materials: ferrites, cobaltites, manganites, doped metallic oxides, illmenites and spinels. On the basis of the published results it is possible to think that the new materials have to be searched inside the lithium doped metallic oxides (Fe, Co, Mn) and $Ln_xM_{1-x}MtO_3$ type perovskites (Ln= lanthanoid element, M=alkaline earths element, Mt=transition element)

In the present work NiO(Li) and $La_xSr_{1-x}CoO_3$ porous cathodes were prepared and characterized in a laboratory scale MCFC. The aim of the experimentation was to determine the reaction orders relative to O_2 and CO_2 for the cathodic reaction and the stability of the materials. To obtain these information a methodology based on electrochemical impedance spectroscopy (EIS) was used.

PREPARATION OF ELECTRODES

The lithium doped nickel oxide, NiO(Li), was obtained starting from a sintered porous nickel. The oxidation and lithiation reactions took place inside the MCFC. The sintered nickel had the following properties: porosity 70%, mean pore diameter 8 μm.

The $La_xSr_{1-x}CoO_3$ (x=0.5÷1) perovskites, in the following called LASCO, were prepared starting from metal acetate solutions, with a defined composition, dried by means of a Buchi mod.190 spray dryer. Then the powders, after calcination, were used to fabricate dense pellets for the electronic conductivity measurements and porous cathodes for in cell electrochemical test.

The La, Sr, Co acetates were dissolved in deionized water at 50°C under mixing for 1 hour; than the solution was dried and the obtained powder, were calcinated up to 550 °C in a quartz crucible in air with an appropriate heat treatment cycle. To optimise the heat treatment, a thermoanalytical study on the precursor powders was carried out; from such an investigation it was pointed out that the acetates decomposition reaction takes place between 270 and 360 °C.

The powders were cold pressed at 100 MPa, in the case of dense pellets, and at 2 MPa for the porous electrodes.

The fabrication of porous structures presented several problems, since the "green" pellets resulted very brittle; therefore it was necessary to use some organic binders. Among several tested binders (metilcellulose, polyvinilic alcohol, paraffin oil, etc.) the best behaviour was showed by metilcellulose in aqueous solution.

The pellets obtained by this procedure, were sintered on a platinum strip (1150 °C, 15 hours). Before this heat treatment, the samples were covered with powder of the same composition to avoid contamination from the furnace and changes in the surface composition.

The electronic conductivity was measured, in air at 650 °C, by means of a d.c. four points probe technique. From XRD measurements it was established that the compound with the higher electronic conductivity (≈ 10^3 S/cm) crystallizes in the rhombohedral system, typical of perovskite compounds, with the following parameters: a=13.19 Å and b=5.45 Å. These values agree with the literature data [24] for the $La_{0.8}Sr_{0.2}CoO_3$ compound.

The LASCO electrodes, fabricated by cold pressing at 2 MPa, had a porosity in the range 45÷55 %, a mean pore diameter of 5 μm, with a bi-modal structure, that is the necessary for an optimal working as MCFC cathode.

EIS MEASUREMENTS

A recristallized alumina MCFC was used to carry out the EIS measurements. The cell was assembled with two identical cathodes (figure 1) instead of the usual configuration

(anode and cathode); such a configuration allows to eliminate the influence of the counter electrode (in this case the anode) and to avoid the use of a reference electrode which is, by itself, a noise source [30].

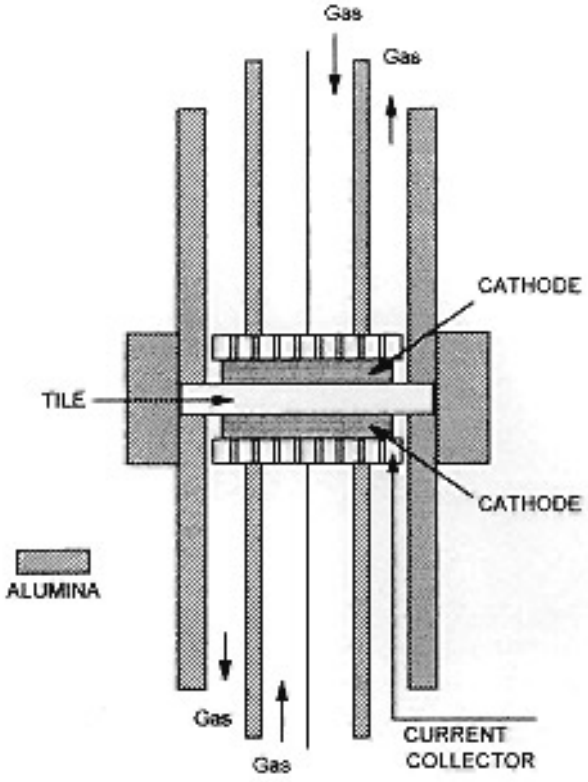

Figure 1 - Schematic view of alumina MCFC with two cathodes.

Two identical porous electrodes with a geometric surface area of 3 cm^2 were used. The tile was fabricated by hot pressing (35 MPa at 495 °C) a mixture of γ-$LiAlO_2$/carbonates (48/52%$_w$); the carbonates were pre-mixed in the eutectic composition (Li/K=62/38 %$_{mol}$). The current collectors were perforated plates made of AISI 316 stainless steel.

The cell was heated at the operative temperature (650±2 °C) with a 30 °C/h ramp, and fed with a variable composition $O_2/CO_2/N_2$ mixture. The measurements were carried out changing the gas composition at a constant gas flow (180 ml/min on both electrodes).

The EIS data were collected by means of a potentiostat-galvanostat Solartron mod.1286 and a frequency response analyser Solartron mod.1250, both controlled by a computer Hewlett Packard mod.310. The cell was galvanostatically polarized with a zero imposed current and a superimposed sinusoidal signal of 236 μA/cm^2 in the frequency range 1 Hz÷65 kHz. The EIS data files were converted from HP BASIC to DOS format by means of an appropriate software running on a HP Vectra ES/12 computer, upgraded with an HP83200B language processor card. This operation was necessary to use a NLLS (non linear least square) software [25]. The experimental set-up is shown in figure 2.

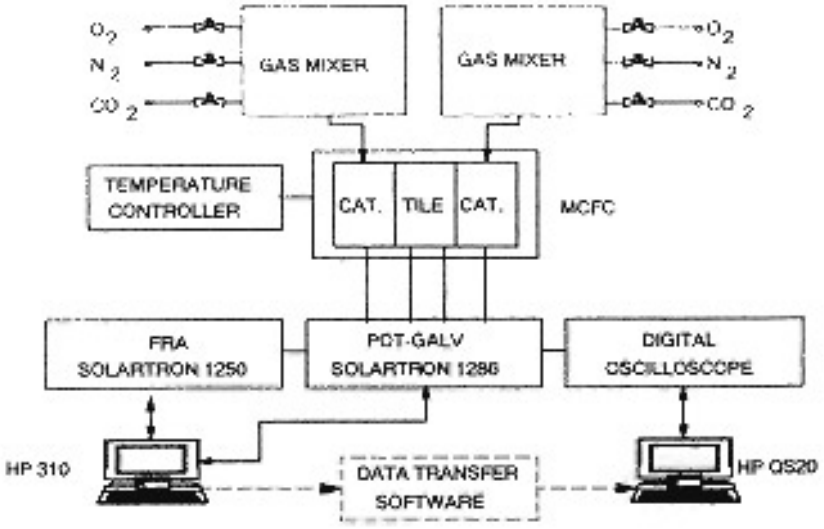

Figure 2 - Experimental set-up

EIS SPECTRA ANALYSIS

A typical EIS spectrum of NiO(Li) at 650 °C is shown in figure 3. This spectrum was recordered after four days from the cell start-up to be sure that the oxidation/lithiation process was completed. At a first look the spectrum is evidently depressed at low frequencies; that means the centre of the circle is located below the real impedance axis, shifted by an α angle.

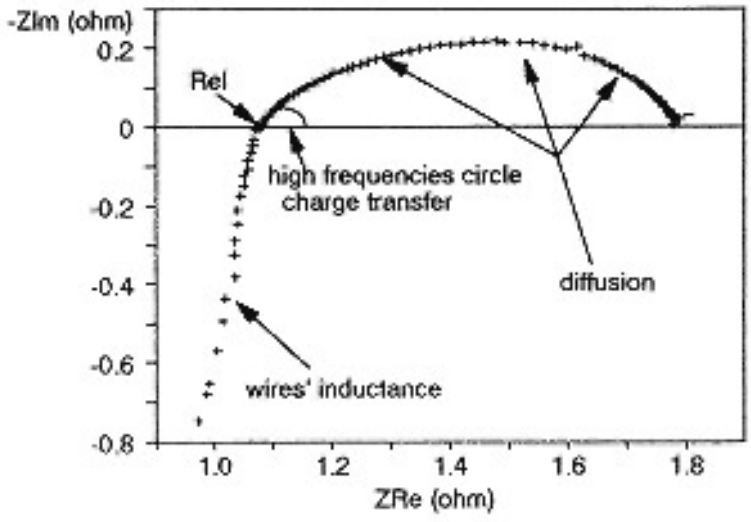

Figure 3 - Typical EIS spectrum of porous NiO(Li) at 650 °C in molten carbonates.

This phenomenon is correlated to the porous electrode structure and is a function of gas composition. The results show that at pressures less than 0.3 atm of CO_2, whatever is the pO_2, the depression angle value is so that the impedance phase angle is less than theoretical value of 22.5° for a porous electrode [14]. Such a condition is verifyed in the case in which $d^2\omega/D<10$, where d is the electrolyte thickness, ω the angular frequency and D the diffusion coefficient of the active species. This unequality is true only when a very thin electrolyte layer is present.

Starting from this point of view, the equivalent electrical circuit for the cathode/electrolyte interface can be simulated by a C(R-CPE) network [26], in which C is the electrochemical double layer capacitance in parallel with the charge transfer resistance (R) and the constant phase element (CPE).

The second evidence is that an inductive component of impedance at high frequencies is present. This interfering phenomenon was correlated to the electrical wires connecting the cell to the measuring instrumentation, and was simulated by a RL series circuit.

To determine the exact contribution of wires to the EIS data, measurements on the short-circuited wires were carried out and it was possible to draw out the following values: L_w=1.45·10^{-6} Henry, R_w=0.02 ohm. Then, we tried to subtract a RL series circuit from the spectra to test these values and we found that the inductance to be subtracted was higher (1.7·10^{-6} Henry) than the measured value. That means that also the cell has an own inductance.

From the data obtained at pCO_2 constant, as pO_2 increases both the total real impedance (TRZ) and the maximum of the immaginary impedance (MIZ) decrease (figure 4a); on the contrary when pO_2 is constant, as pCO_2 increases both TRZ and MIZ increase (figure 4b). An increase of TRZ has as consequence a slow down of the kinetic and diffusive processes, while a change in MIZ value means a change on the interfacial condition of the electrode.

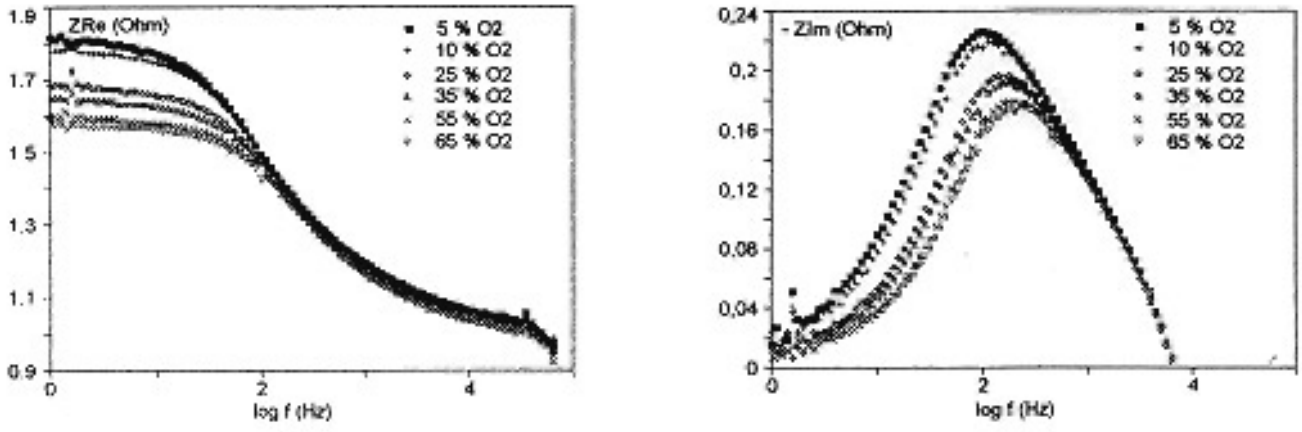

Figure 4a - Dependency of real and imaginary impedance component on pO_2.

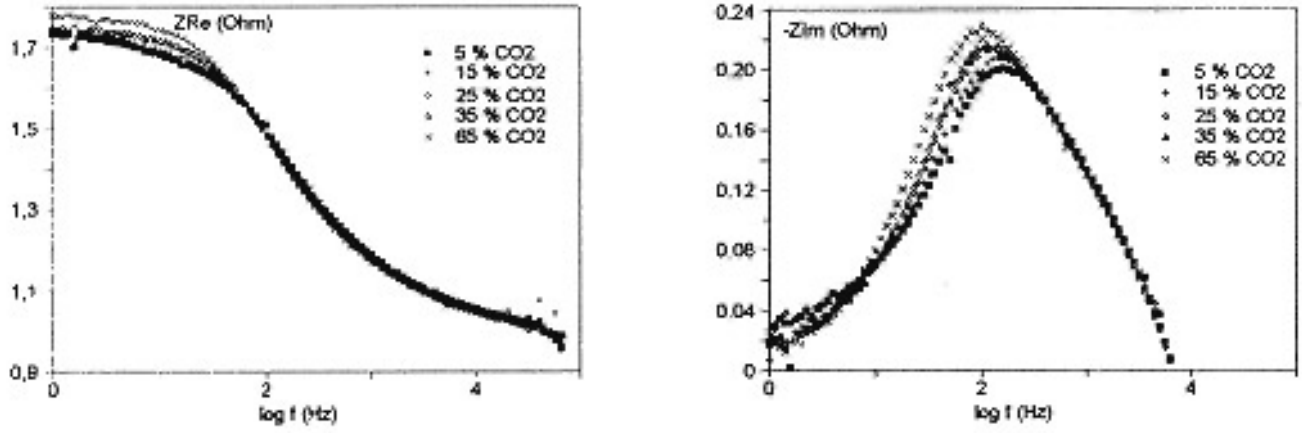

Figure 4b - Dependency of real and imaginary impedance component on pCO_2.

As consequence it can be concluded that: the pO_2 has a positive influence on the cathodic reaction, while the pCO_2 has a negative influence. These results are in good agreement with the mechanisms reported in literature, in which the exchange current density has a positive dependency on pO_2 and a negative one on pCO_2 (table 1).

Using a geometrical algorithm it is possible to translate the spectrum to obtain the EIS data without the depression at low frequencies. After this operation the spectrum has the aspect shown in figure 5a. In the same figure is reported also the simulation of a spectrum relative to a semi-infinite diffusion layer to demonstrate that in MCFC we are in presence of a finite diffusion layer, i.e., the diffusion layer and the electrolyte thickness are coincident and therefore the active species gradient is localized inside the whole electrolyte. That means that the electrode pores are not flodded, but coated with a very thin electrolyte layer [30]. Such a spectrum can be deconvoluted as shown in figure 5b. To obtain this second shape the circuit code and the equivalent circuit shown in figure 5b were used [30, 31].

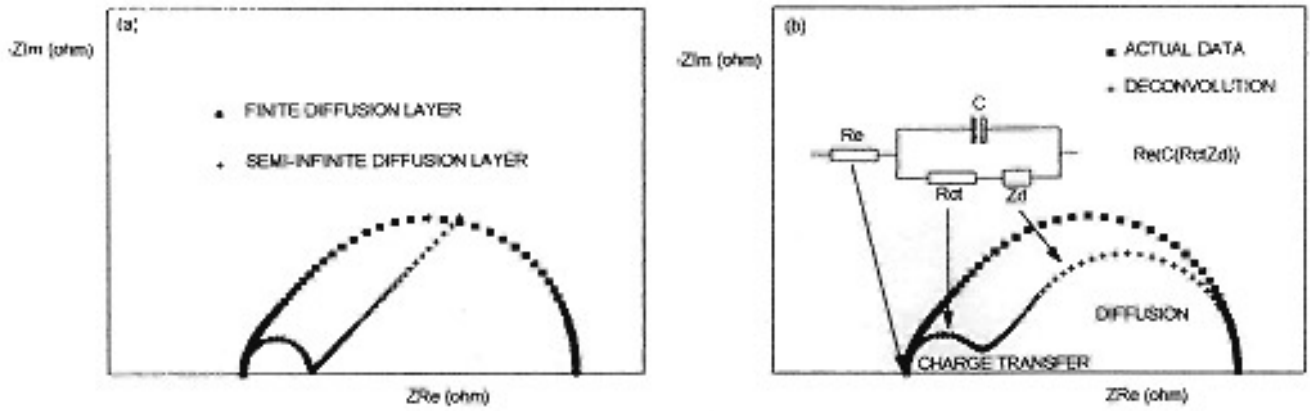

Figure 5 - Simulation of different conditions for the diffusion layer (a) and deconvolution in the case of finite diffusion layer (b).

The deconvoluted spectra can be subdivided in two regions: low-medium frequencies in which the diffusion is predominant and high frequencies in which the charge transfer phenomena are predominant. In fact the equivalent circuit that gave the best fitting results for the interface was a network made up with a charge transfer resistance (R_{ct}), a double layer capacitance (C) and a characteristic element [25] of a system in which is present a finite diffusion layer :

(8) $$Z_d(\omega) = \tanh [B(j\omega)^{0.5}]/[Y^{\circ}(j\omega)^{0.5}]$$

in which B and Y° are two parameters containing the diffusion coefficient of the reactant species, the film thickness and other coefficients related to the system. The fact that the electrode/molten carbonates interface can be simulated by means of a R_{ct}, C and Z_d elements, it is a confirmation that the pores of the cathode are not completely flooded: the pore walls are coated by a thin film of electrolyte and the concentration gradient of active species extends completely to the film thickness.

A typical EIS spectrum for the LASCO perovskite is shown in figure 6, recorded just after the achievement of the operative temperature.

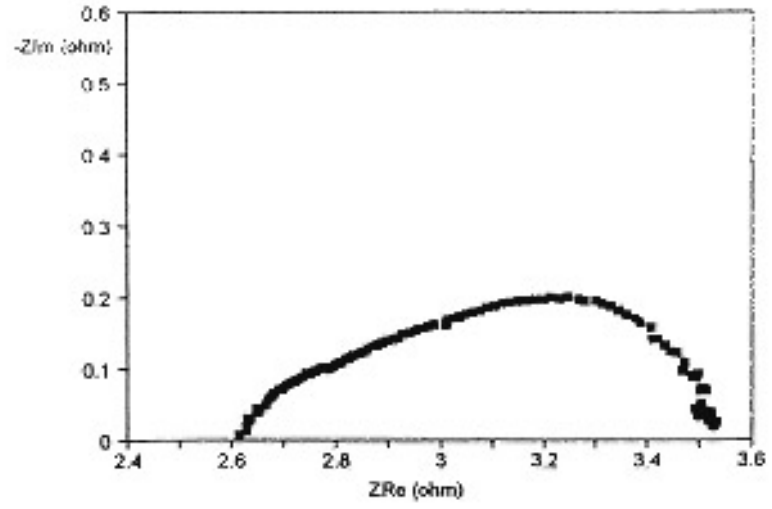

Figure 6 - EIS spectrum of $La_{0.2}Sr_{0.8}CoO_3$ recorded after 22 h from the warm-up of the cell (T=660 °C, pO_2=0.14 atm, pCO_2=0.30 atm, pN_2=0.56 atm).

Such a frequency dispersion can be described, as in the case of NiO(Li), by the equivalent circuit showed in figure 5. The frequency dispersion is the result of two different phenomena: the mass transport at medium-low frequencies and the charge transfer at higher frequencies.

REACTION ORDERS FOR O_2 ELECTROREDUCTION

As already stated, two main features characterize the spectra: a low frequencies region dominated by diffusion and a high frequencies region in which the kinetic aspect is predominant. This latter is related to the interphase processes and by its analysis the value of charge transfer resistance (R_{ct}), which is inversely proportional to the partial pressures of O_2 and CO_2, can be obtained. In fact, the exchange current density is given by

(9) $$i_o = RT/nFR_{ct}$$

and from equation (7):

(10) $$1/R_{ct} = k\ pO_2^a\ pCO_2^b$$

Following Yuh [15] and Makkus [27] the R_{ct} value can be extracted by the maximum of imaginary impedance component. Using this methodology we did not found any correlation between R_{ct} and the partial pressure of CO_2 and O_2.

As a first approach the R_{ct} values can be derived from the diameter of not depressed high frequencies circle (figure 3), which is proportional to the square root of charge transfer resistance of an equivalent flat electrode [14,15]. Following this methodology we did not find any correlation between the R_{ct} values and the gas composition. That is probably due to the very low numeric values of the R_{ct} compared to the total impedance, which reflect in a very high error and dispersion on R_{ct} value.

The problems arising from the high frequencies fit were overcome by using a non linear least square fit (NLLSF) [25,28] made on the whole spectrum. By this methodology we obtained the equivalent circuit and the circuit code shown in figure 7, which is able to simulate the experimental data with a low relative errors. The Q elements in the circuit represent a constant phase element $Z_Q=(j\omega)^{-n}/Yo$, in which the n exponent is less than 1 for low frequencies (Q_{lf}) and about 1 for high frequencies (Q_{hf}).

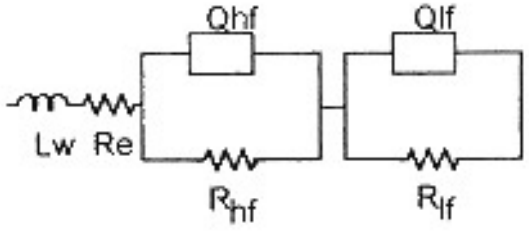

Figure 7 - Equivalent electrical network and circuit code for the EIS data of figure 3. [Lw: wires inductance, Re:electrolyte resistance, R: high (hf) and low (lf) frequencies resistance, Q: high (hf) and low (lf) frequencies constant phase element]

The two (RQ) terms are relative to interfacial phenomena which are difficult to understand from a physical point of view. It is necessary to consider that a good fit result do not necessary has a physical meaning for the global equivalent circuit. In fact several circuits are able to simulate the same EIS data. Therefore the circuit of figure 7 does not necessary represent the global interfacial conditions, but it is only the simpler mathematical approximation of the interface.

In any case, a good correlation between log R_{hf} and log pO_2, log pCO_2 was found. That means the R_{hf} term can be associated to the R_{ct} parameter. In our case (porous electrode), the relationship between R_{hf} and R_{ct} is expressed by:

(13) $$R_{hf} \approx R_{ct}^{0.5}$$

and as consequence

(14) $$1/R_{hf}^2 \approx pO_2^a pCO_2^b$$

Keeping constant the partial pressure of a gas, it is possible to derive the reaction order relative to the other gas. As an example, at constant pCO_2 we can obtain:

(15a) $$\log R_{hf} = -1/2 \log k' - a/2 \log pO_2$$

A similar relationship can be obtained in the case of constant pO_2:

(15b) $$\log R_{hf} = -1/2 \log k'' - b/2 \log pCO_2$$

Therefore from the slope of the previous equations it is possible to draw out the reaction orders (the results are summarized in table 2). It is clear that the reaction orders present a good reproducibility, especially in the case of pO_2 dependency.

Tab.2- Reaction orders calculated after a total fit of the spectra.

pO_2 (atm)	pCO_2 (atm)	a	b	r
0.10÷0.60	0.10	0.38±0.12		0.91
0.05÷0.65	0.30	0.36±0.06		0.91
0.14	0.05÷0.65		-0.91±0.21	0.93
0.50	0.05÷0.50		-1.16±0.12	0.98

The mean experimental reaction order relative to O_2 is 0.37±0.09 and therefore it is very close to the theoretical value both for POP and POMCP mechanisms (0.375). On the contrary, the mean reaction order relative to CO_2 is 1.04±0.17; such a value is four time higher than POMCP mechanism (-0.25) and intermediate to SOP (-0.75) and POP (-1.25) mechanism.

Consequently, it was difficult to exactly assign a mechanism, also because the mean fitting error is high (>10%).

The results clearly point out that the R_{ct} values obtained in such a way are greatly affected by the medium-low frequencies portion of the spectra, related to the diffusion phenomena. Therefore, in order to get a more reliable correlation the medium-low frequencies data points were subtracted from the spectra and a high frequencies fitting was carried out [31].

The following procedure was adopted:

a) subtraction of wires' inductance;
b) simulation of (RQ) circuit at medium-low frequencies;
c) medium-low frequencies fit with the (RQ) circuit;
d) subtraction of (RQ) from the spectrum;
e) simulation with a R(RQ) of the remaining data;
f) final fit with R(RQ) circuit on the remaining data.

Adopting such a procedure the fitting errors were low (<5%), and a very good correlation between log R_{ct} values and partial pressures of O_2 and CO_2 was obtained (figure 8).

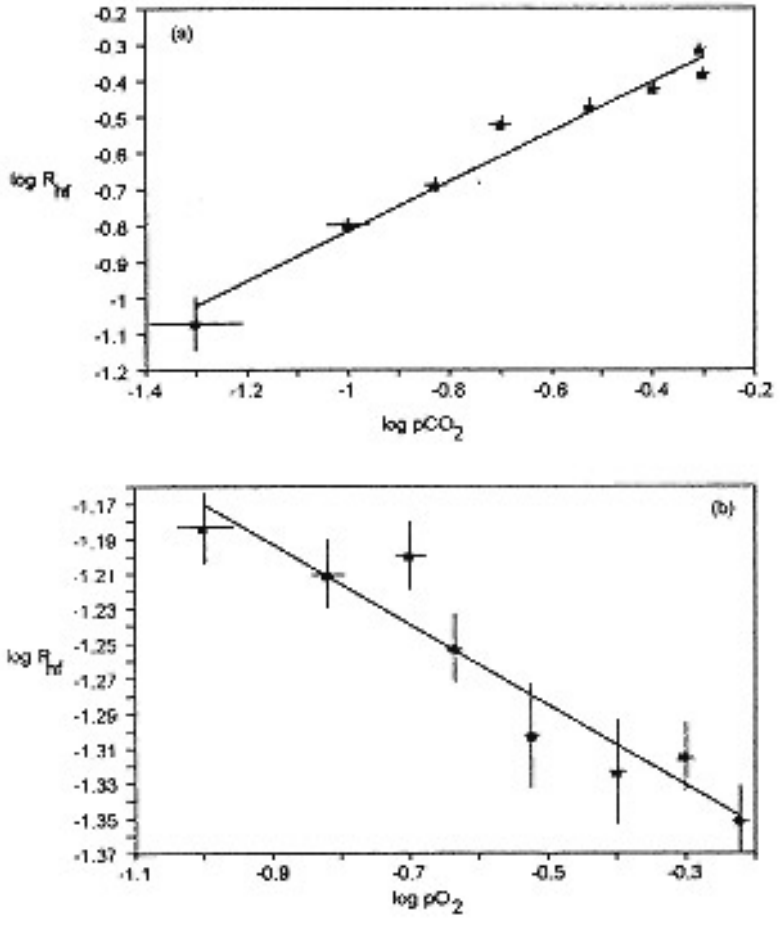

Figure 8 - Log-log correlation between the high frequencies resistance (network of figure 5) and the partial pressure of carbon dioxide (a) and oxygen (b).

From the dependency of charge transfer resistance on gas composition, the reaction orders relative to O_2 and CO_2 were determined by means of equations (15a) and (15b).

The data obtained from different series of measurements, made on two different cells, are shown in table 3

Table 3- Reaction orders calculated after a partial high frequencies fit of the spectra.

pO_2 (atm)	pCO_2 (atm)	a	b	r
0.10÷0.60	0.10	0.30±0.08		0.96
0.10÷0.60	0.30	0.44±0.08		0.94
0.05÷0.65	0.30	0.36±0.09		0.91
0.14	0.10÷0.60		-1.37÷0.23	0.95
0.14	0.05÷0.65		-1.28÷0.20	0.97
0.50	0.05÷0.50		-1.38÷0.14	0.98

The mean calculated reaction orders are: a=0.37±0.08 and b=-1.34±0.19. These results are in good agreement with the theoretical values for the peroxide mechanism, particularly in the case of oxygen reaction order.

A series of measurements at pCO_2=0.10 atm and pCO_2=0.30 atm on LASCO electrodes were carried out; then the measurements were carried out at pO_2=0.14 atm and pO_2=0.30 atm. The dependency of the spectra shape on gas mixture composition in a short time (quasi-stationary conditions for several hours) follows the foreseen theoretical behaviour, just confirmed on NiO(Li) electrodes. In fact the total polarisation resistance (R_p) and the maximum of the imaginary impedance component ($-Zim_{max}$) decrease with pO_2 and increase with pCO_2 (fig.9).

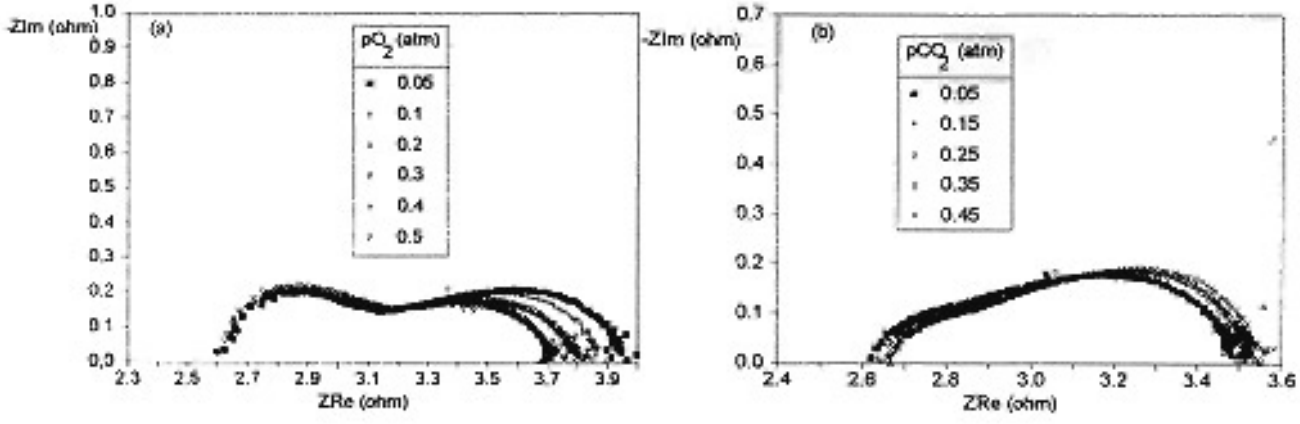

Figure 9 - Influence of gas composition on the LASCO spectra in the case of pCO_2=0.30 atm (a) and pO_2=0,30 atm (b).

The same spectra analysis methodology used for NiO(Li) was applied to LASCO data and the results are summarized in table 4. It is clear that the values are not reproducible and they do not agree with any of the proposed mechanisms for the electroreduction of O_2/CO_2 mixture in molten carbonates (table 1).

Table 4 - Calculated reaction orders for O_2/CO_2 electroreduction on LASCO.

pO_2 (atm)	pCO_2 (atm)	a	b
0.10÷0.60	0.10	0.62±0.12	
0.10÷0.60	0.30	0.29±0.06	
0.14	0.10÷0.60		-0.15±0.13
0.30	0.10÷0.60		-0.25±0.03

STABILITY OF NiO(Li) AND LASCO

The NiO(Li) has a good stability in molten carbonates, in presence of a cathodic gas mixture, as a function of time (figure 10), and therefore it is possible to follow the kinetic changes, if they occurs.

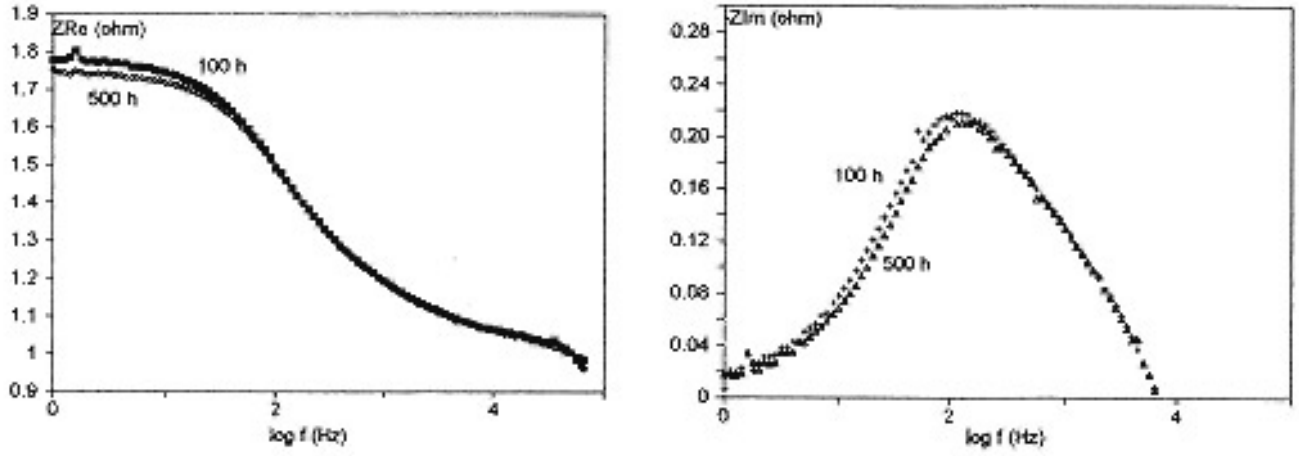

Figure 10 - Stability of NiO(Li)/molten carbonates interface after 100 and 500 hours from the cell start-up.

By following the time evolution of the spectra shape, for the LASCO electrodes, the figure 11 was obtained. While the electrolyte resistance is time invariant, the interfacial phenomena are subjected to considerable changes. Particularly, after 200 h the total polarisation resistance (R_p) becomes twice its value and above 100 Hz a very large semicircle appears; this loop was related to a new phenomenon overlapping the diffusion and reactive processes. In such a situation the equivalent circuit proposed for NiO(Li) is not yet valid, but it is necessary to add another time constant.

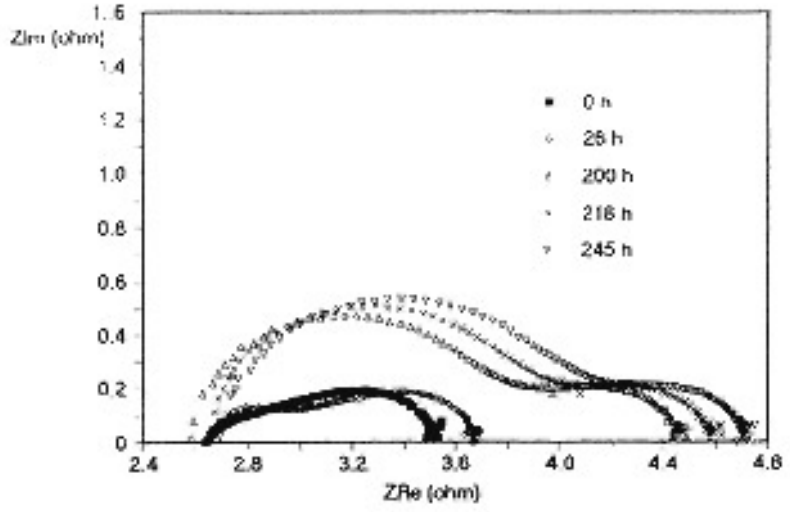

Figure 11 - Time changes of the LASCO spectra shape.
(T=650 °C, pO2=0.14 atm, pCO2=0.30 atm)

Analysing the behaviour of the imaginary impedance component as a function of frequency and time (figure 12) we can point out that just after 26 h, the high frequencies loop begins to be evident. That induces to think that the system evolves very quickly. Therefore, it is not possible to study the O_2/CO_2 electroreduction kinetic due to the instability of the electrode/electrolyte interface and the anomalous data of table 4 can be view under another perspective.

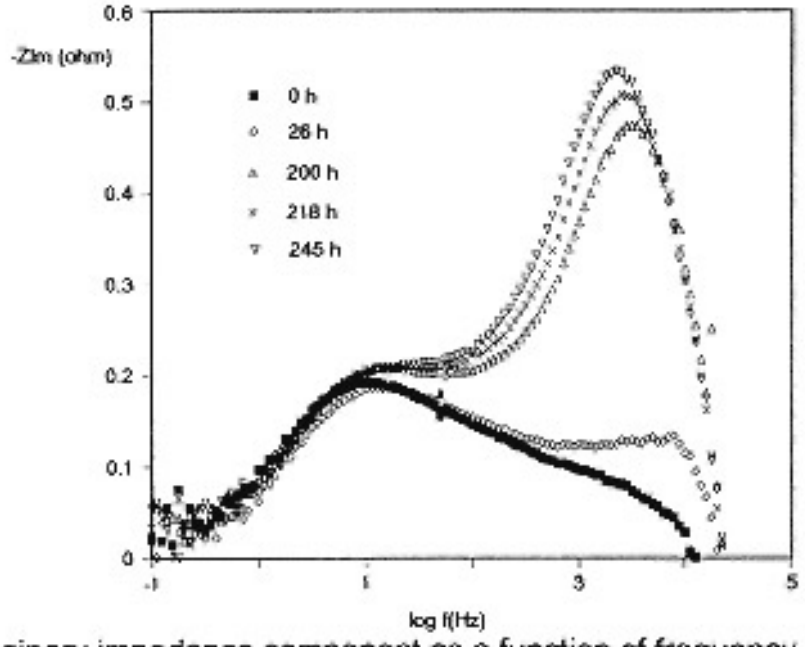

Figure 12 - Imaginary impedance component as a function of frequency and time for the LASCO electrodes (T=650 °C, pO_2=0,14 atm, pCO_2=0,30 atm).

The determination of the R_{ct} values, as explained before, was difficult due to the presence of the high frequencies loop which hides the charge transfer process. The dimension of the high frequencies loop is not a function of the O_2/CO_2 mixture composition and so it can not be correlated to a charge transfer phenomenon. The nature of the physical-chemical processes to which the high frequencies phenomena, totally absent in the case of lithium doped nickel oxide, are due, never was studied up to date, neither by researchers who

investigated the electrochemistry of a La, Sr, Co perovskite [29] or their stability in MCFC [23].

In the EIS spectrum some characteristic parameters can be underlined (figure 13), which can help to understand the interfacial phenomena.

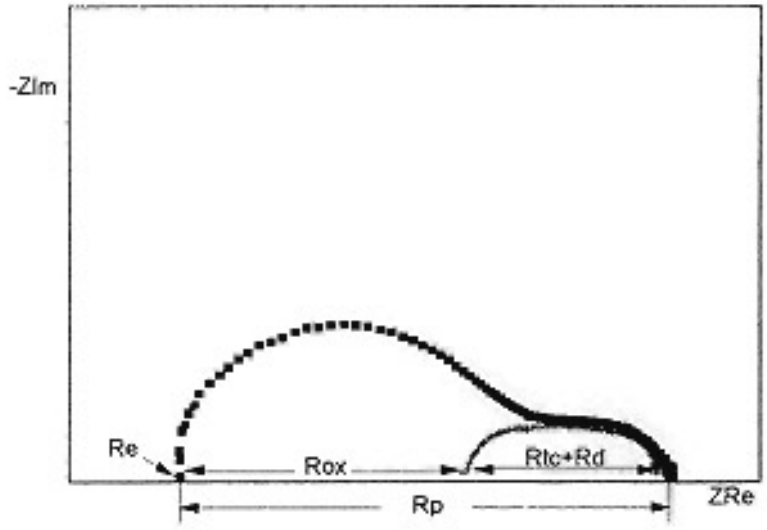

Figure13 - Real impedance parameters drawn out from LASCO spectra (Re: electrolyte resistance, Rox: oxide resistance, Rp: total polarization resistance, Rct: charge transfer resistance, Rd: diffusional resistance).

Since the high frequencies loop becomes larger by the time (figure 12), it was hypotized that the phenomenon is relative to passivation processes, as in the case of lithium electrodes in polimeric electrolyte batteries [33]. To understand if the latter hypothesis is valid the passivating film was reduced by means of a galvanostatic cycling ($i=\pm$ 300 mA/cm^2 for 3 minutes). Making a comparison between the EIS spectra before and after the galvanostatic treatment (figure 14) it is clear that the passivating film was largely destroyed or reduced and that is a confirmation of its presence.

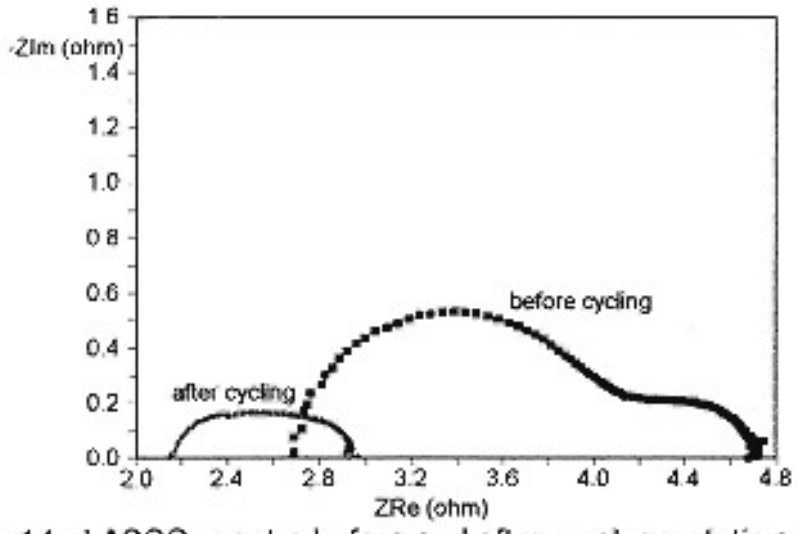

Figure 14 - LASCO spectra before and after a galvanostatic cycling.

After the electrochemical treatment the R_p value is reduced by 50 % and the electrolyte resistance (R_e) by 20 %. The slow down of R_p and R_e can be correlated with the reduction of passivating film and, particularly, we can deduce that the oxide layer, grown on the electrode surface, has both ionic and electronic conductivity. In fact the R_e slow down suggests that such a parameter is the sum of two contributes: the molten carbonates and the oxide film resistance.

A confirmation of the presence of a dynamic film on the electrode surface is furnished by the figure 15, in which are shown the EIS spectra as function of time, after the previous described reduction treatment. The R_e values grow again, while the sum of diffusive (R_d) and reactive (R_{ct}) impedance is quite constant (figure 16). This is a confirmation that only the growing process is time dependent.

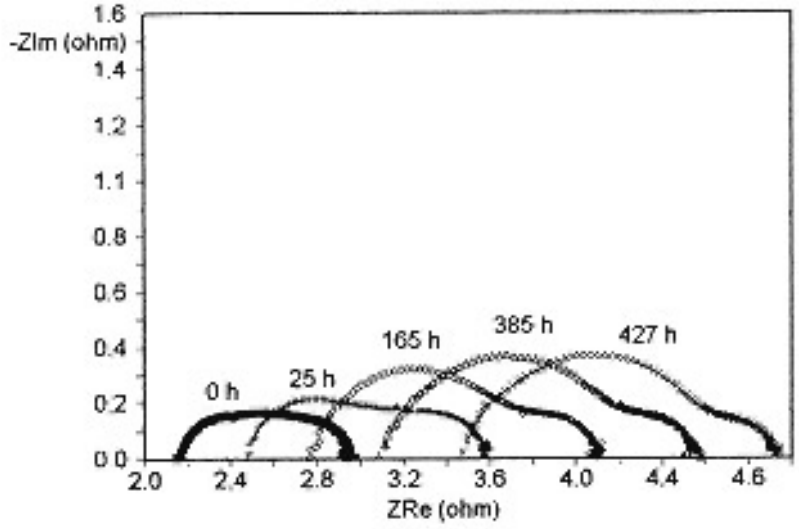

Figure 15 - Time changes of LASCO spectra after a galvanostatic cycling.

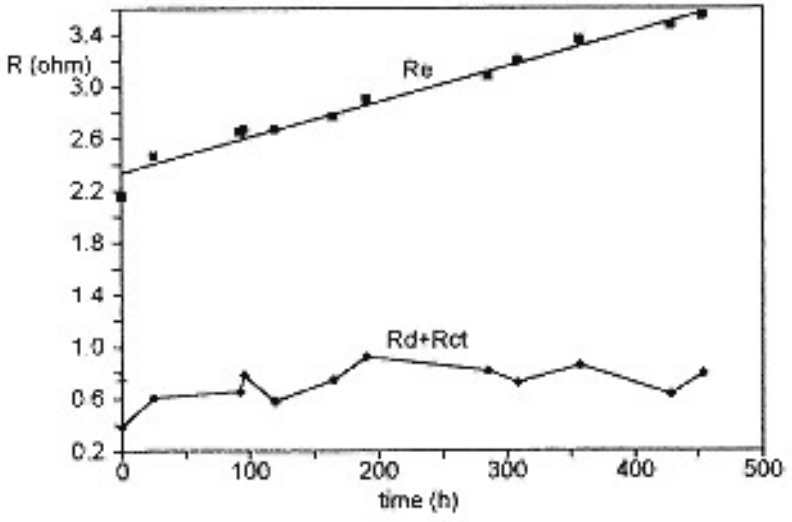

Figure 16 - Time changes of the electrolyte resistance (R_e) and sum of diffusional (R_d) and charge transfer resistance (R_{ct}).

CONCLUSIONS

The NiO(Li) electrode, not considering the dissolution of Ni^{2+}, is very stable in molten alkaline carbonates from a point of view of the interfacial electrode/electrolyte characteristics. For this reason it is possible to determine the reaction orders relative to O_2 and CO_2 for the oxygen electroreduction, and it was found that the peroxide mechanism is the most favoured in Li_2CO_3/K_2CO_3 eutectic mixture at 650 °C. Moreover, the existance and stability of peroxide ions in molten Li_2CO_3/K_2CO_3 was recently confirmed by Moutiers et al. [34] by means of thermodynamic and voltammetric analysis

The EIS measurements have put in evidence a long term instability of $La_{0.8}Sr_{0.2}CoO_3$ in molten carbonates; in fact the material becomes passive with a consequent increase of the total impedance. It seems that the passive film growth does not influence the electrode kinetic (mass and charge transfer).

Several hypothesis can be done to give an explanation of the formation of the passive film and the increase of R_e with time. R_e can increases because the lithium ion of the electrolyte enters into the perovskite lattice by means of an intercalation process; therefore the electrode/electrolyte interface is depleted in Li^+ and, as a consequence, the conductivity is reduced. Another possible cause can be the slow down of the electrode conductivity. In fact, the strontium is the dopant element in the perovskite, therefore a reduction in the concentration of Sr^{2+} in the lattice leads to a lower electronic conductivity. The loss of Sr^{2+} ions from the electrode is very probable, because of the high affinity between earth-alkaline elements and molten carbonates.

A further explanation of the electrode instability is a reaction between the perovskite and the ceramic of the tile:

(16) $$LaCoO_3 + LiAlO_2 \Rightarrow LaAlO_3 + LiCoO_2$$

The reaction products are a not conductive ($LaAlO_3$) and a conductive ($LiCoO_2$) compound. The $LaAlO_3$ could be the responsable for the electrode passivation (high frequencies loop). The $LiCoO_2$ is one of the possible alternative materials for MCFC cathodes; the problem for its use as a cathode is that the stoichiometric compound has a low conductivity, while a defective one has a conductivity very close to that of NiO(Li) [32]. Therefore, an increase of Re value can be ascribed to the formation of a not very conductive lithium cobaltite, which, together the lanthanum aluminate, reduces the total conductivity of the LASCO electrodes.

ACKNOWLEDGEMENTS

The authors would like to acknowledge Dr. M. Patriarca for the electronic conductivity measurements and Mr. F. Pallini for the technical support in the experimental work.

REFERENCES

1) Maru, H., Farooque, M., Paetsch, I., Yuh, C., Patel, P., Doyon, J., Bernard, R.: Proc. of 1992 Fuel Cell Seminar, p.29, November 29-December 2, 1992, Tucson (USA)
2) Ottervanger, R., Boersma, R., de Vaal, L.: Proc. of 1992 Fuel Cell Seminar, p.31, November 29-December 2, 1992, Tucson (USA)
3) Hiari, C.,Matsumura,M., Gonjo, Y., Sasaki, A., Nishiyama, E.: Proc. of 1992 Fuel Cell Seminar, p.61, November 29-December 2, 1992, Tucson (USA)
4) Proc. of 1992 Fuel Cell Seminar, p.61, November 29-December 2, 1992, Tucson (USA)
5) Appleby, A.J., Nicholson, S.B.: J. Electrochem. Soc., 1980, 127,759
6) Appleby, A.J., Nicholson, S.B.: J. Electroanal. Chem., 1977, 83, 309

7) Nishina, T., Uchida, I.: Denki Kagaku, 1988, 56, 419
8) Uchida, I., Nishina, T., Mugikura, Y., Itaya, K.: J. Electroanal Chem., 1986, 206, 229
9) Nishina, T., Uchida, I.: Denki Kagaku, 1988, 56, 419
10)Nishina, T., Lindbergh, G., Kudi, T., Uchida, I.: Proc. of International Fuel Cell Conference, p.193, 3÷6 February, 1992, Makuhari (Japan).
11)Giorgi, L., Simonetti, E., Pozio, A.: Proc. of 2nd International Symposium on Electrochemical Impedance Spectroscopy, 11÷17 July, 1992, S. Barbara (USA).
12)Makkus, R.C., Weever, R., Hemmes, K., de Wit, J.H.W : J. Electrochem. Soc., 1990, 137, 3154
13)Tryk, D.A., Yeager, E.B.: Proc. of Molten carbonate Fuel Cell Technology, The Electrochem. Soc. Proc. Vol. 90-16, Pennington, N.J., 1990
14) de Levie, R.:Electrochim. Acta,1964, 9, 1231
15)Selman, J.R., Yuh, C.Y.: J. Electrochem. Soc. 1992, 138, 3649
16)Shores, D.A., Selman, J.R., Israni, S., Ong, E.T.:Proc. of Molten carbonate Fuel Cell Technology, The Electrochem. Soc. Proc. Vol. 90-16, Pennington, N.J., 1990
17)Orfield, M.L., Shores, D.A., J. Electroche. Soc., 1989, 136, 2862
18)Doyon, J.D., Gilbert, T., Davies, G.: J. electrochem. Soc., 1987, 134, 3035
19)Baumgartner, C.E.: J. Electrochem. soc., 1984, 131, 1850
20) Baumgartner, C.E., Arendt, R.H., Iacovangelo, C.D., Karas, B.R.: J. Electrochem. Soc., 1984, 131, 2217.
21)Brown, A., Kucera, G., Roche, M., Chu, D., Indachochea, E.: Proc. of 1992 Fuel Cell Seminar, p.25, November 29÷December 2, 1992, Tucson (USA)
22)Bergman, B., Fontes, E., Lindbergh, G., Largergren, C., Lundblod, A.: Proc. of 1992 Fuel Cell Seminar, p.73, November 29÷December 2, 1992, Tucson (USA)
23)Chun, H., Lim, J., Park, K., Kim, K.: Proc. of 1992 Fuel Cell Seminar, p.571, November 29÷December 2, 1992, Tucson (USA)
24)Ohbayashi, H., Kudo, T., Gejo, T.: Jpn. J. Appl. Phys., 1974, 13, 1
25)Boukamp, B.A.: EQUIVCRT.PAS, Users Manual, 1988
26)Giorgi, L., Simonetti, E., Gavelli, G.:Proc. of NATO-ASI "Electrified Interfaces in Physics, Chemistry and Biology", p.16, Varenna (Italy), 23th July÷3rd August, 1990
27)Makkus, R.: Thesis, Technische Universiteit, Delft, 1991
28)Boukamp, B.A.: Solid State Ionics, 1986, 20, 31
29)Franke, M., Winnick, J.: J. Appl. Electrochem., 1989, 19,1
30)Pozio, A.: Thesis, University of Rome, December, 1991
31)Giorgi, L., Simonetti, E., Pozio, A.: Proc. of 1992 Fuel Cell Seminar, p.554, November 29÷December 2, 1992, Tucson (USA)
32) Carewska, M., Giorgi, L., Patriarca, M., Scaccia, S., Simonetti, E., Di Bartolomeo, A.: 3rd Groove Fuel Cell Symposium, London, 28 September÷1 October, 1993
33) Capuano, F., Croce, F., Scrosati, B.: J. Electrochem. Soc.,1991, 138, 1918
34) Moutiers, G., Cassir, M., Devynck, J.: J. Electroanal. Chem., 1992, 324, 175